

Strain accumulation due to packages of cycles with varying amplitude and/or average stress - on the bundling of cycles and the loss of the cyclic preloading memory

T. Wichtmannⁱ⁾ Th. Triantafyllidisⁱⁱ⁾

Abstract: In order to predict permanent deformations by means of a high-cycle accumulation (HCA) model, a random cyclic loading, i.e. a loading with frequently changing amplitudes, has to be grouped into packages of cycles each with a constant amplitude. Based on a series of drained triaxial tests on fine sand, in which the same cycles have been applied either in an order with frequently changing amplitudes or in packages of cycles, it is demonstrated that such bundling is conservative. Predictions by the HCA model of Niemunis et al. [19] are confronted with experimental data and with other approaches for the prediction of permanent deformations under packages of cycles, among them the frequently cited procedure of Stewart [26]. An effect not captured in the HCA model or in any other approach yet has been detected in another series of tests with a change of the average stress between bundles of cycles: The monotonic loading associated with this change can partially or fully erase the memory of the sand regarding its cyclic preloading history.

Keywords: Drained cyclic triaxial tests; random cyclic loading; packages of cycles; high-cycle accumulation model; erasure of cyclic preloading memory

1 Introduction

In many practical problems with high-cyclic loading, i.e. a loading with a large number of cycles $N > 10^3$ with relatively small to moderate strain amplitudes $\varepsilon^{\text{amp}} < 10^{-3}$, the amplitude of the cycles changes frequently. For example, foundations of offshore wind power plants (OWPP) are subjected to such random cyclic loading caused by wind and waves. In order to predict the permanent deformations of the OWPP foundations, e.g. by means of a high-cycle accumulation (HCA) model as that proposed by Niemunis et al. [19], it is necessary to group the cycles into a limited number of packages each with an (almost) constant amplitude (Figure 1). The packages can then be treated sequentially. However, such bundling would be only allowed if the original random order of amplitudes generates the same final residual strain as the same cycles when ordered into packages. A respective experimental examination with drained cyclic triaxial tests is documented in Section 2.

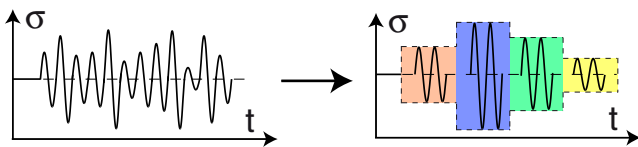


Fig. 1: Bundling of a random order of amplitudes into packages of cycles

Several approaches for the prediction of permanent deformations of shallow foundations or piles due to packages

ⁱ⁾Researcher, Institute of Soil Mechanics and Rock Mechanics, Karlsruhe Institute of Technology, Germany (corresponding author). Email: torsten.wichtmann@kit.edu

ⁱⁱ⁾Professor and Director of the Institute of Soil Mechanics and Rock Mechanics, Karlsruhe Institute of Technology, Germany

of cycles as those shown on the right-hand side of Figure 1 have been proposed in the literature. The most popular one is that of Stewart [26], which nowadays is frequently cited in the literature dealing with OWPP foundations for the North sea [1, 10, 11, 27]. In Section 3 this approach is confronted with the prediction of the HCA model of Niemunis et al. [19] and with experimental results. Other less suitable procedures [4, 17] are also briefly addressed.

In all experimental studies with packages of cycles presented in the literature so far, the average stress has been kept constant during the entire test procedure. In contrast, Section 4 presents a study with changes of the average stress between consecutive packages of cycles. These tests are of practical relevance for OWPP foundations too, since beside the amplitude also the average value of the wind and wave loading frequently changes. Based on the results of these new tests an effect not captured in any procedure for packages of cycles yet has been discovered: The memory of the sand regarding its cyclic preloading history can be partially or fully erased by the monotonic loading caused by the changes of the average stress.

An irregular cyclic stress or strain history is also caused by an earthquake. For a liquefaction risk analysis, it is usually converted into an equivalent number of uniform cycles, i.e. a single package of cycles with constant amplitude. Respective procedures and experimental studies with undrained cyclic loading are described e.g. in [2, 6–8, 12, 18, 21–24, 28, 29]. The present paper, however, concentrates on a drained high-cyclic loading.

2 Comparison of tests with frequently changing amplitudes and packages of cycles

The tests dealing with the question whether a bundling of a random cyclic loading is allowed or not have been per-

formed on Karlsruhe fine sand (fines content $FC \approx 0\%$, mean grain size $d_{50} = 0.14$ mm, uniformity coefficient $C_u = 1.5$, minimum void ratio $e_{\min} = 0.677$, maximum void ratio $e_{\max} = 1.054$, grain density $\rho_s = 2.65$ g/cm³). The medium dense samples were prepared by dry air pluviation using a funnel. The average stress was the same in all tests (average mean pressure $p^{\text{av}} = 200$ kPa, average stress ratio $\eta^{\text{av}} = q^{\text{av}}/p^{\text{av}} = 0.75$, with $p = (\sigma'_1 + 2\sigma'_3)/3$ and $q = \sigma'_1 - \sigma'_3$). The cyclic loading was applied with a loading frequency of 0.1 Hz in the axial direction while the lateral stress has been kept constant. The four stress amplitudes $q^{\text{ampl}} = 20, 40, 60$ and 80 kPa were applied with 12,500 cycles each. The total number of cycles was thus 50,000 in all tests.

The sequence of the stress amplitudes has been varied (Figure 2a). Four load types with frequently changing amplitudes (upper row of schemes in Figure 2a) and four other ones with packages of cycles (lower row in Figure 2a) have been tested. In test type No. 1 the amplitudes were modulated, i.e. applied in an order similar to a wavelet signal. Four cycles with increasing amplitude (20 → 40 → 60 → 80) were followed by four other ones with descending order (80 → 60 → 40 → 20). 6250 of these wavelets were applied in succession. In test type No. 2 the bundle of four cycles with ascending order of amplitudes (20 → 40 → 60 → 80) was applied 12,500 times. Type No. 3 was similar to type No. 2, but the order of amplitudes was chosen as 40 → 80 → 20 → 60. In the last type of test with frequently changing amplitude (type No. 4) eight cycles with the sequence 20 → 20 → 40 → 40 → 60 → 60 → 80 → 80 were repeated 6,250 times. In case of the load types Nos. 5 to 8 (Figure 2a) the cycles were grouped to four or eight packages with 12,500 or 6,250 cycles of equal amplitude, respectively. These packages were applied in ascending or descending order. Usually, a single test with $0.58 \leq I_{D0} = (e_{\max} - e)/(e_{\max} - e_{\min}) \leq 0.65$ was performed for each type of load signal. Only the signal types 2 and 5 were studied in an additional test at a slightly higher relative density $I_{D0} \approx 0.7$.

As outlined in [19, 35, 38] the first cycle of a bundle of cycles may lead to larger residual deformations than the subsequent ones, because the first quarter of the cycle (or some part of this first quarter) represents a first loading. Therefore, the first cycle is sometimes termed *irregular*. The HCA model describes the residual strain accumulation due to the subsequent *regular* cycles only. In the tests of types Nos. 1 - 4 (Figure 2a) a single cycle with an amplitude $q^{\text{ampl}} = 80$ kPa and a lower loading frequency of 0.01 Hz was applied prior to the 50,000 cycles with frequently changing amplitudes, in order to anticipate the portion of residual strain caused by the first loading. The sample deformations caused by this first cycle are not further used in this paper. In case of the tests with packages of cycles (types Nos. 5 - 8 in Figure 2a), each package with 6,250 or 12,500 cycles was preceded by a single cycle with the same amplitude as the following bundle. Also the deformations caused by these first cycles are not included in the further analysis of residual strains. Only the data from the *regular* cycles being of relevance for the HCA model are discussed in the following.

Figure 2b presents the measured development of total residual strain ε^{acc} (with $\varepsilon = \sqrt{(\varepsilon_1)^2 + 2(\varepsilon_3)^2}$) with increasing number of cycles N in the eight tests with $0.58 \leq I_{D0} \leq 0.65$. In order to purify the data from the influ-

ence of the slightly different initial densities, in Figure 2c the residual strain ε^{acc} has been divided by the void ratio function f_e of the HCA model (see equations in Appendix A), which was evaluated with the initial void ratio e_0 for simplicity reasons. Obviously, all tests with signals of types 1 to 4, i.e. with a frequently changing amplitude, deliver a similar residual strain $\varepsilon^{\text{acc}}/f_e(e_0)$ after 50,000 cycles, irrespective of the order of the amplitudes. The tests with cycles grouped into four or eight packages (types 5 to 8) even lead to somewhat larger residual strains at the end of the test (Figure 2c). This is also evident in Figure 2d where the final residual strain after 50,000 cycles has been plotted versus the initial relative density I_{D0} . It can be concluded that the bundling of cycles with frequently changing amplitudes into a limited number of packages with constant amplitudes leads to somewhat higher residual deformations than in case of the original signal, i.e. the bundling procedure may be regarded as conservative. Furthermore, Figure 2e reveals, that the direction of strain accumulation, i.e. the direction of the $\varepsilon_v^{\text{acc}} - \varepsilon_q^{\text{acc}}$ strain paths ($\varepsilon_v = \varepsilon_1 + 2\varepsilon_3 =$ volumetric strain, $\varepsilon_q = 2/3(\varepsilon_1 - \varepsilon_3) =$ deviatoric strain) is rather unaffected by the order of the amplitudes.

3 HCA model prediction vs. approaches for packages of cycles proposed in the literature

The prediction of the HCA model for packages of cycles has been discussed in detail in [35, 38]. Due to its preloading variable g^A (see the equations in Appendix A) the HCA model is able to reproduce the strain accumulation curves $\varepsilon^{\text{acc}}(N)$ measured in tests with packages of cycles applied at constant average stress. Figure 3 presents respective examples. In those six tests on a medium dense, medium coarse sand four packages with 25,000 cycles each and stress amplitudes $q^{\text{ampl}} = 20, 40, 60$ and 80 kPa were applied in different sequences. A good agreement between the curves resulting from simulations with the HCA model (blue solid curves in Figure 3) and the experimental data can be concluded. The HCA model approximately obeys Miner's rule [16], i.e. the sequence of the packages is of minor importance regarding the final residual strain. This is in good accordance with both the experimental results in Figure 3 and other respective studies in the literature [3, 9, 14, 26].

For the prediction of residual deformations due to packages of cycles with different amplitudes, the approach of Stewart [26] is frequently addressed in the literature and recommended for practical applications [1, 4, 10, 11, 27]. The procedure proposed by Stewart [26] is shown schematically in Figure 4, for three packages of cycles with increasing amplitude. The approach is explained in terms of the residual strain ε^{acc} in an element test with cyclic loading, instead of a horizontal pile head deflection y or a foundation settlement s as it can be frequently found in the literature. In contrast to the HCA model, Figure 4 assumes an accumulation obeying $\varepsilon^{\text{acc}} \sim N^a$, but the approach is applicable to any shape of the accumulation curve. The procedure is shown in diagrams with both a linear (Figure 4a) and a log-log scale (Figure 4b).

Three accumulation curves, each corresponding to a freshly pluviated sample and identical values of void ratio and average stress, but three different amplitudes 1, 2 and 3 are given in Figure 4. After N_1 cycles with the smallest amplitude 1 a residual strain $\varepsilon_1^{\text{acc}}$ remains in the soil. This residual strain is converted into an equivalent number of cy-

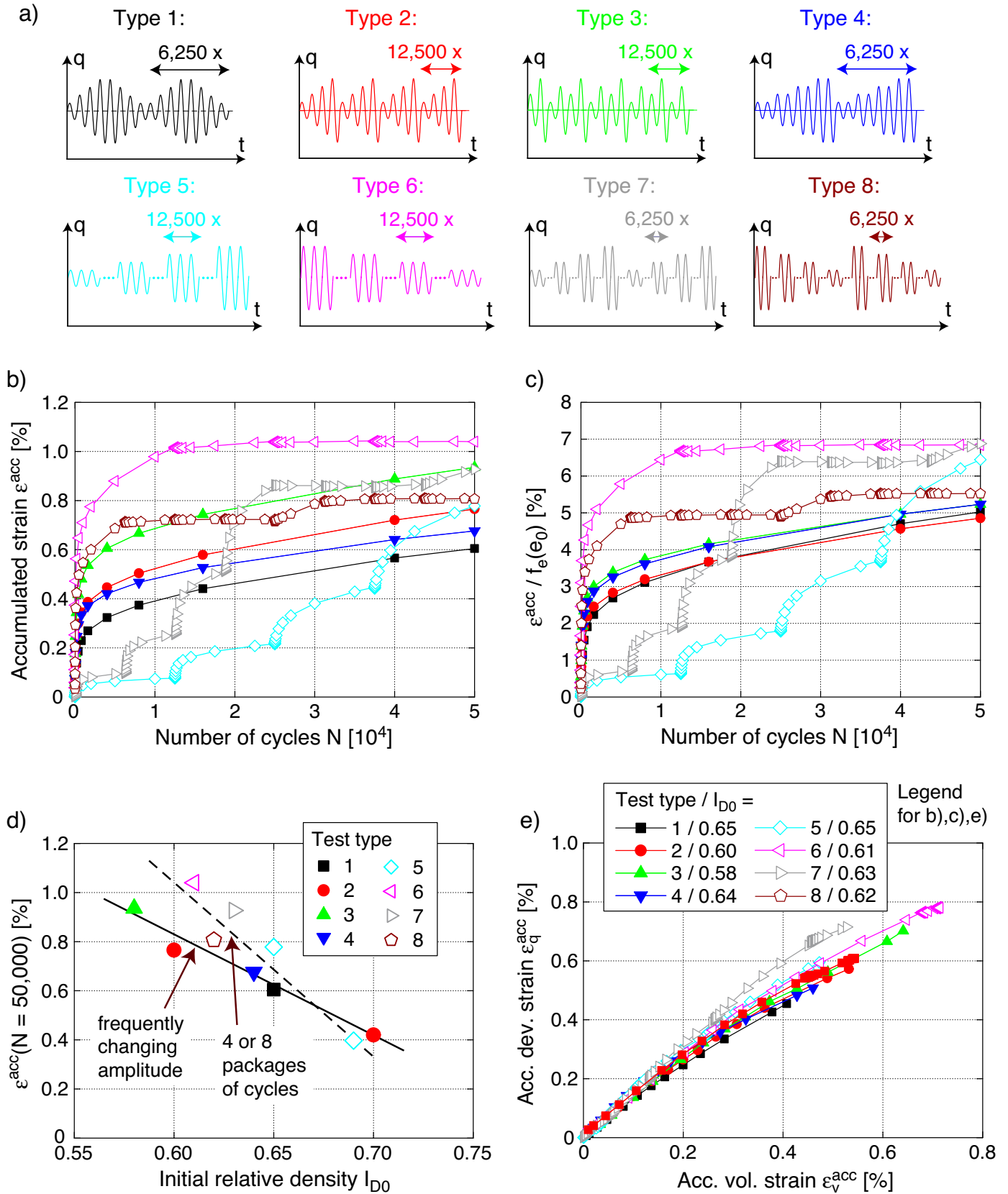


Fig. 2: Comparison of tests with frequently changing amplitude and tests with the same cycles applied in four or eight packages: a) Tested cyclic load signals, b) Accumulated strain ϵ^{acc} as a function of the number of cycles N , c) $\epsilon^{acc}(N)$ divided by void ratio function $f_e(e_0)$ of the HCA model, d) Residual strain after 50,000 cycles versus initial relative density I_{D0} , e) $\epsilon_v^{acc} - \epsilon_q^{acc}$ strain paths. Only the residual strains caused by the regular cycles are shown (data from first irregular cycle of each package are excluded).

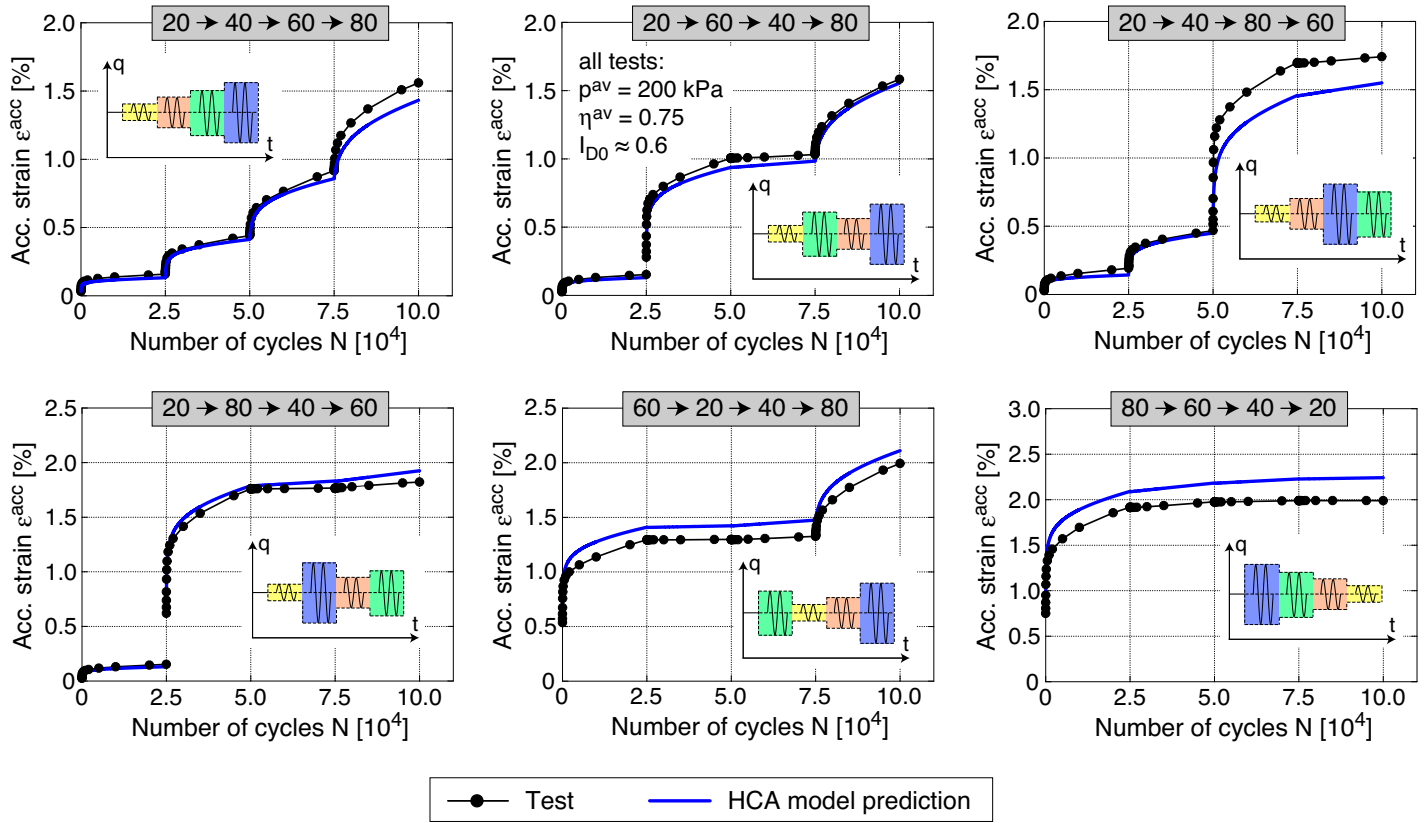


Fig. 3: Accumulation of residual strain in drained cyclic triaxial tests with packages of cycles applied at constant average stress. The four amplitudes ($q^{ampl} = 20, 40, 60$ and 80 kPa) were applied in six different sequences (see gray boxes). The experimental results are compared to the prediction by the HCA model [35, 38].

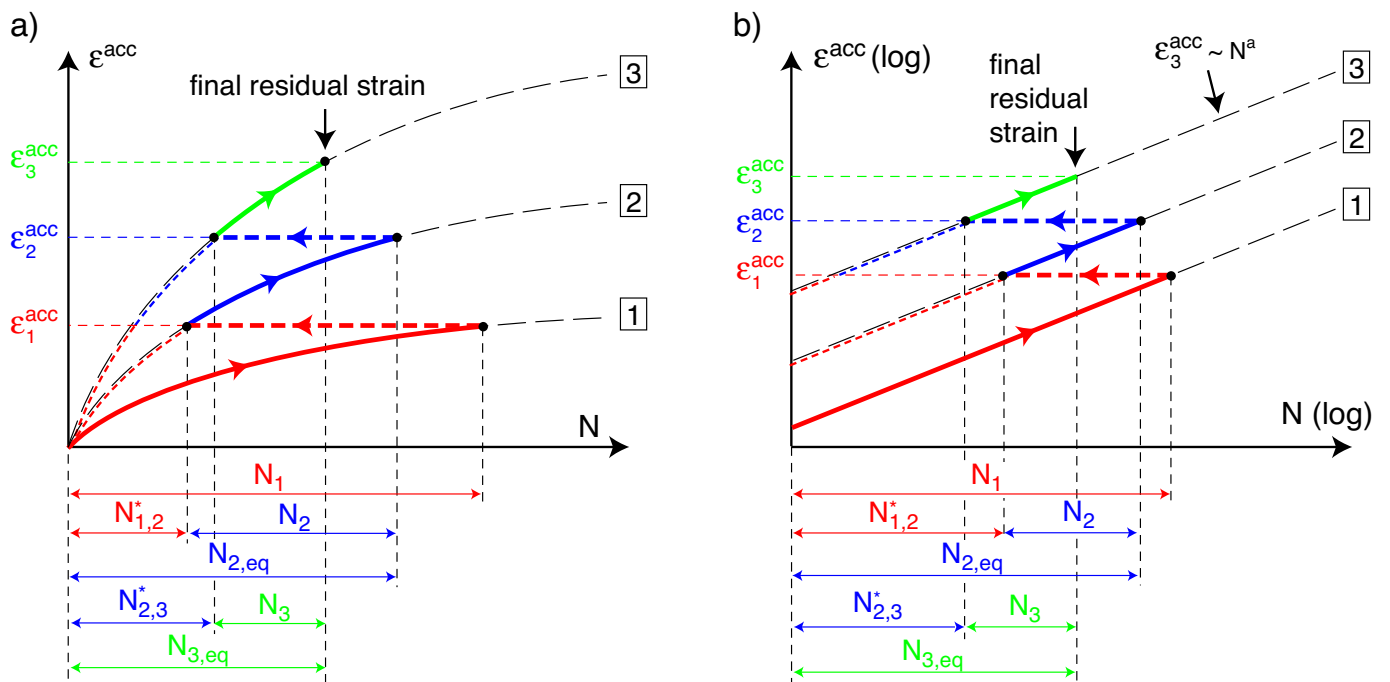


Fig. 4: Procedure for packages of cycles proposed by Stewart [26], illustrated with a) linear or b) log-log scale of the axes

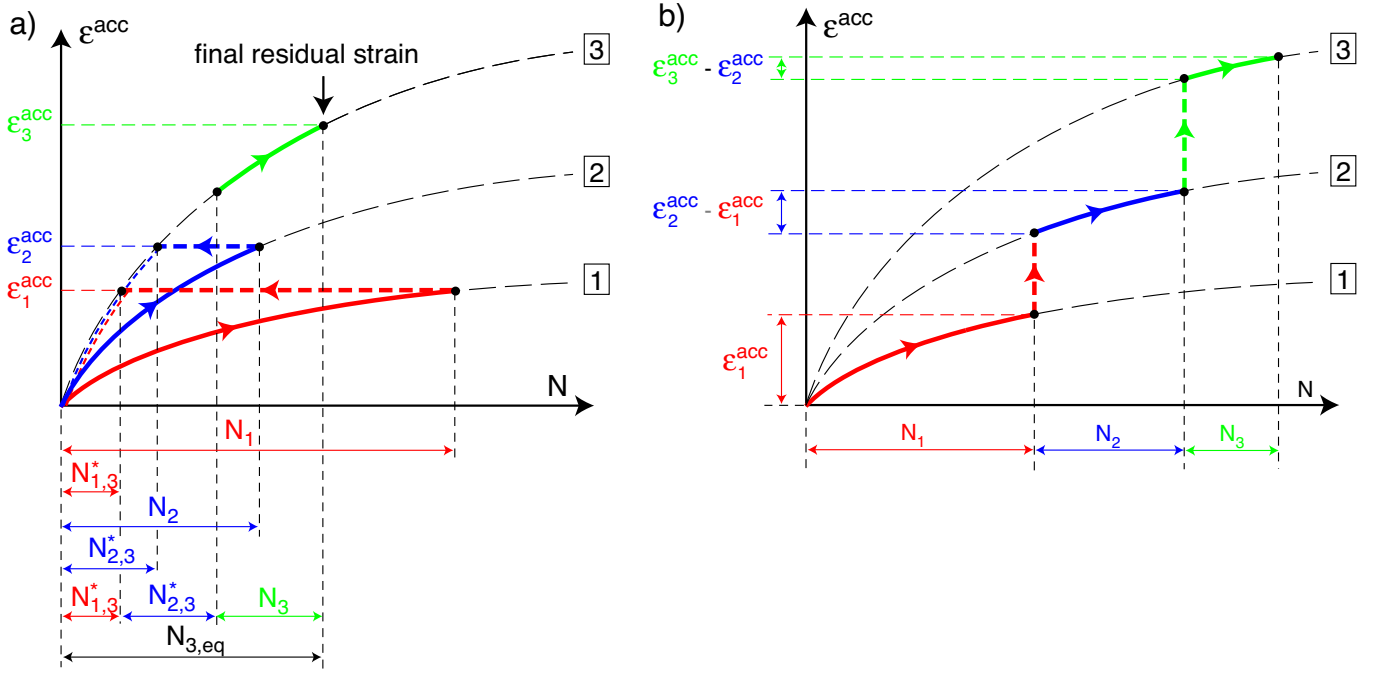


Fig. 5: a) Graphical representation of the equations proposed in the German recommendations for piles "EA Pfähle" [4], b) Schematic drawing of the "Strain Hardening" method proposed by Monismith et al. [17]

cles $N_{1,2}^*$ for amplitude 2 of the second package of cycles, i.e. $N_{1,2}^*$ cycles with amplitude 2 cause the same residual strain as N_1 cycles with amplitude 1. This conversion corresponds to a horizontal projection of the point $(N_1, \varepsilon_1^{\text{acc}})$ lying on curve 1 into the point $(N_{1,2}^*, \varepsilon_1^{\text{acc}})$ on curve 2. The cyclic preloading due to the first package of cycles is considered in the calculation of the accumulation due to the second package with N_2 cycles, i.e. the calculation starts from the point $(N_{1,2}^*, \varepsilon_1^{\text{acc}})$ and follows the curve 2 up to the point $(N_{2,\text{eq}}, \varepsilon_2^{\text{acc}})$ with $N_{2,\text{eq}} = N_{1,2}^* + N_2$. Subsequently, the residual strain $\varepsilon_2^{\text{acc}}$ is converted into an equivalent number of cycles $N_{2,3}^*$ referring to amplitude 3, corresponding to a horizontal projection of the point $(N_{2,\text{eq}}, \varepsilon_2^{\text{acc}})$ into the point $(N_{2,3}^*, \varepsilon_2^{\text{acc}})$ on curve 3. Finally, starting from this point N_3 cycles with amplitude 3 are calculated, leading to the final residual strain $\varepsilon_3^{\text{acc}}$ at $N_{3,\text{eq}} = N_{2,3}^* + N_3$. In a similar manner the procedure can be applied to packages of cycles with descending amplitude.

The described procedure is applied either to the accumulated portion of deformation only (e.g. [10,11]) or to the total deformation, comprising also the deformation due to static loading and due to the first cycle (e.g. [13,27]). Formulas for the equivalent numbers of cycles $N_{1,2}^*$, $N_{2,3}^*$ and the residual strains $\varepsilon_1^{\text{acc}}$, $\varepsilon_2^{\text{acc}}$ and $\varepsilon_3^{\text{acc}}$, assuming either a power law relationship $\varepsilon^{\text{acc}} \sim N^a$ or a logarithmic function $\varepsilon^{\text{acc}} \sim 1 + a \ln(N)$ are provided in Appendix B.

The equations in the German recommendations for piles "EA Pfähle" [4] (see Appendix C), used e.g. for OWPP monopile foundations under their cyclic horizontal loading do not obey the concept of Stewart [26]. The procedure proposed in [4] is shown schematically in Figure 5a. The comparison with Figure 4 reveals that the equations in [4] do not correctly consider the cyclic preloading. For example, the effect of the cyclic preloading due to the preceding N_1 cycles with amplitude 1 is not considered when calcu-

lating the residual strain $\varepsilon_2^{\text{acc}}$ due to N_2 cycles with amplitude 2. As shown by example calculations in [39], using the equations in [4] the final residual deformation depends on the chosen reference amplitude, i.e. on the sequence of the packages. Therefore, Miner's rule is not fulfilled.

The "Strain Hardening" method proposed by Monismith et al. [17] (mentioned also in [27], see the scheme in Figure 5b) is inappropriate as well, since it considers the cyclic preloading only by the number of cycles, disregarding their amplitude. Both approaches illustrated in Figure 5 cannot be recommended for practical applications.

Next, the prediction by the HCA model will be compared with the approach of Stewart [26]. Figure 6 presents an example in which the development of residual strain due to three packages of cycles with an increasing sequence of amplitudes ($N_1 = 10,000$, $N_2 = 5,000$, $N_3 = 1,000$, $\varepsilon_1^{\text{ampl}} = 2 \cdot 10^{-4}$, $\varepsilon_2^{\text{ampl}} = 4 \cdot 10^{-4}$, $\varepsilon_3^{\text{ampl}} = 6 \cdot 10^{-4}$) has been calculated "by hand" using the equations of the HCA model along with the approach of Stewart [26] as illustrated in Figure 4. The equations of this example are given in detail in Appendix D. The calculation results in a final residual strain of $\varepsilon_3^{\text{acc}} = 0.738\%$. The curve $\varepsilon^{\text{acc}}(N)$ generated with the procedure according to Stewart [26] is also shown as dashed curve in Figure 7. The result for a descending order of the same amplitudes is given in Figure 7 as well. The dashed curves in Figure 7 are almost identical with the solid curves which have been obtained from element test calculations with the full HCA model. Based on Figure 7 it can be concluded that the HCA model equations approximately implement the approach of Stewart [26]. Furthermore, Figure 7 once again confirms that the HCA model approximately obeys Miner's rule.

The by-hand calculation according to Stewart [26] presented in Figures 6 and 7 reproduces the residual strain predicted by the HCA model only approximately. In Ap-

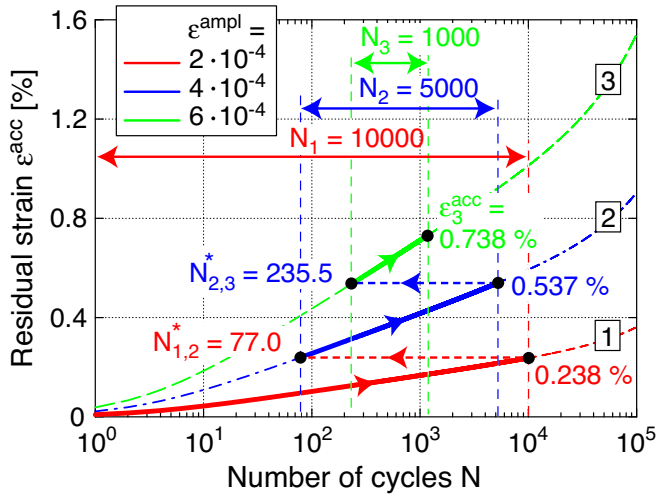


Fig. 6: "By hand" calculation of the residual strain due to three packages of cycles with increasing amplitude, using the HCA model equations and the approach of Stewart [26]

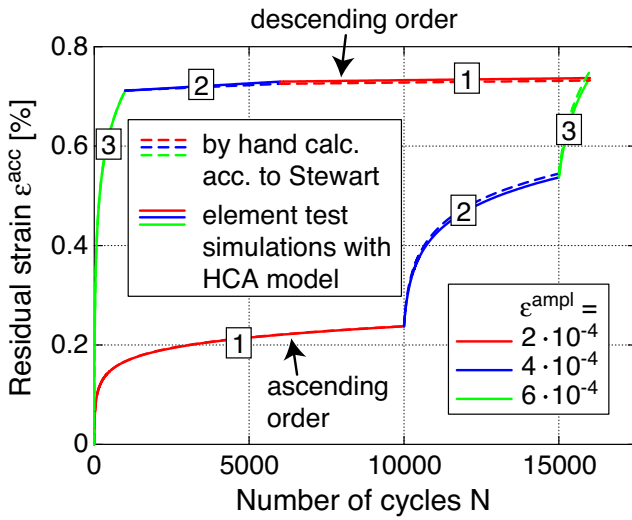


Fig. 7: Comparison of the curves $\varepsilon^{\text{acc}}(N)$ obtained from the "by hand" calculation according to Stewart [26] (Figure 6) and from element test simulations with the full HCA model

pendix E the exact equations for a by-hand calculation of packages of cycles using the HCA model are given.

4 Tests with a variation of average stress between packages of cycles - Erasure of cyclic preloading memory

The series of tests presented in this Section have originally been performed in order to check if the HCA model parameters can be calibrated from multi-stage tests, i.e. tests with a subsequent application of packages of cycles at various average stresses and with different stress amplitudes. Such multi-stage tests were expected to reduce the experimental effort necessary for the calibration of the HCA model. However, as demonstrated in the following, the test results revealed an unexpected erasure of cyclic preloading memory not considered in the HCA model or in any other approach for the handling of packages of cycles yet.

A natural fine sand taken near-shore in Cuxhaven, Germany has been used in these experiments ($FC = 0\%$, d_{50}

$= 0.10$ mm, $C_u = 1.6$, $e_{\min} = 0.612$, $e_{\max} = 0.947$, $\rho_s = 2.65$ g/cm³). First, the HCA model parameters of this sand were calibrated from 17 single-stage drained cyclic triaxial tests with different stress amplitudes q^{ampl} , initial relative densities I_{D0} , average mean pressures p^{av} and average stress ratios η^{av} . All samples were prepared by dry air pluviation and subjected to 100,000 regular cycles with a loading frequency of 0.2 Hz. The regular cycles were preceded by an irregular cycle with the same amplitude but a lower loading frequency of 0.01 Hz. The data of the irregular cycle is not further used herein. The strain accumulation curves $\varepsilon^{\text{acc}}(N)$ measured in the four test series during the regular cycles are presented in Figure 8, along with the prediction of the HCA model using the optimum parameters summarized in Table 1. Obviously, the intensity of strain accumulation grows with increasing values of amplitude (Figure 8a), average mean pressure (Figure 8c) and average stress ratio (Figure 8d) while it decreases if the sand becomes denser (Figure 8b). The experimental and numerical data agree well, confirming a good prediction quality of the HCA model.

φ_{cc} [°]	C_{ampl} [-]	C_e [-]	C_p [-]	C_Y [-]	C_{N1} [10 ⁻⁴]	C_{N2} [-]	C_{N3} [10 ⁻⁴]
32.6	1.07	0.37	0.01	2.04	4.38	0.103	0.091

Table 1: HCA model parameters of Cuxhaven fine sand

In a second step, four multi-stage tests on medium dense ($0.62 \leq I_{D0} \leq 0.65$) air-pluviated samples have been performed. Figure 9a shows the development of accumulated strain ε^{acc} with increasing number of cycles N in a test similar to those already presented in Figure 3, i.e. with cycles applied at a constant average stress ($p^{\text{av}} = 200$ kPa, $\eta^{\text{av}} = 0.75$). The four packages with 25,000 cycles each and stress amplitudes $q^{\text{ampl}} = 20, 40, 60$ and 80 kPa were applied in ascending order, using a loading frequency of 0.2 Hz. Figure 9a presents the development of residual strain with N during the regular cycles. The experimental data agree well with those presented in Figure 3 and similar test series in the literature [9,26,35,38]. $\varepsilon^{\text{acc}}(N)$ data stemming from a recalculation of this test using the HCA model with the parameters calibrated from the 17 single-stage tests are shown as red curve in Figure 9a. Due to its preloading variable g^A the HCA model is able to reproduce the measured curve $\varepsilon^{\text{acc}}(N)$ satisfactorily.

In the three other multi-stage tests the average stress has been monotonically changed between the successive packages of cycles. Similar as in the first test, each package comprised 25,000 cycles with a loading frequency of 0.2 Hz. These cycles were preceded by an irregular cycle of same amplitude but lower frequency (0.01 Hz). In the second test (Figure 9b) the average stress ratio $\eta^{\text{av}} = 0.75$ was kept constant while the average mean pressure was increased from $p^{\text{av}} = 100$ kPa over 200 kPa to 300 kPa. The amplitude-pressure ratio was chosen as $q^{\text{ampl}}/p^{\text{av}} = 0.3$ in all three packages. A variation of the average stress ratio was investigated in the third and fourth test (Figure 9c,d). The average mean pressure $p^{\text{av}} = 200$ kPa and the stress amplitude $q^{\text{ampl}} = 60$ kPa were kept constant in both tests. Five packages of cycles at $\eta^{\text{av}} = 0, 0.5, 0.75, 1.0$ and 1.25 were applied in Test No. 3, while the sample of test No. 4 was subjected to three bundles at $\eta^{\text{av}} = 0, 0.75$ and 1.25

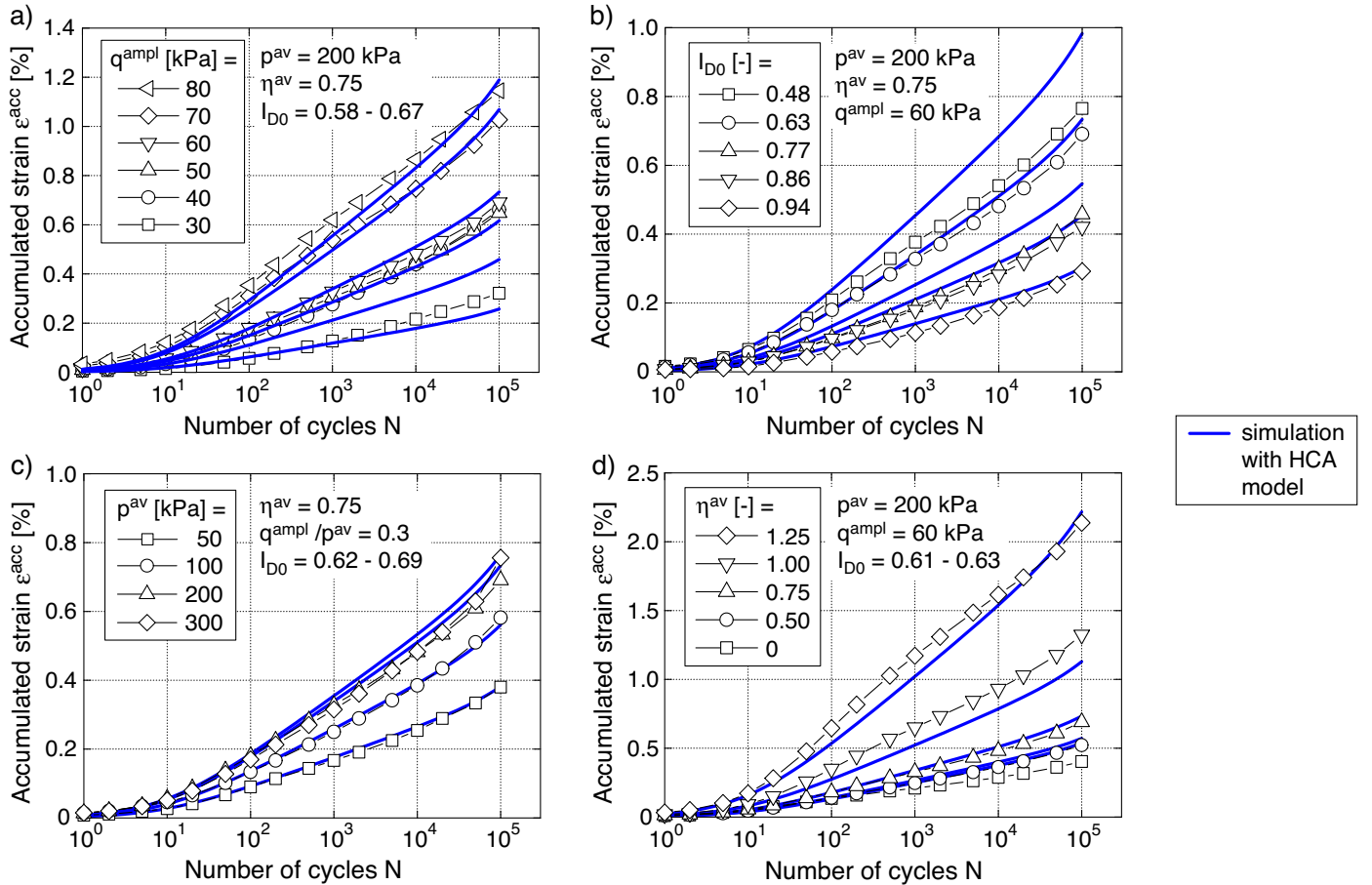


Fig. 8: Strain accumulation curves $\varepsilon^{acc}(N)$ measured in tests on Cuxhaven fine sand with varying a) stress amplitudes q^{ampl} , b) initial relative densities I_{D0} , c) average mean pressures p^{av} and d) average stress ratios η^{av} . Only the residual strains caused by the regular cycles are shown (data from first irregular cycle are excluded). The prediction by the HCA model using the parameters in Table 1 has been added as blue curves.

only. The curves of residual strain development during the regular cycles provided in Figure 9b-d exhibit a significant increase of the rate of strain accumulation at the beginning of each new package of cycles.

The results of simulations of tests Nos. 2 to 4 with the HCA model using the parameters calibrated from the single-stage tests have been added as red curves in Figure 9b-d. Obviously, the strain accumulation rates measured in the later packages of these three tests are significantly underestimated by the HCA model. This is in contrast to the simulations of the single-stage tests, where the pressure- and stress ratio-dependence experimentally observed could be adequately reproduced (Figure 9c,d). Therefore, the differences between the experimental results and the model prediction apparent in Figure 9b-d must be due to an effect not captured by the HCA model yet.

The drained cyclic loading leads to subtle changes in the orientations of the grains or grain contacts, usually rendering the sand fabric more stable to the subsequent cycles, i.e. leading to an adaption of the fabric to the actual cyclic loading and thus to a reduction of the strain accumulation rate $\dot{\varepsilon}^{acc}$ with increasing number of cycles. In the HCA model this is phenomenologically captured by the preloading variable g^A . In the multi-stage tests presented in Figure 9b-d the change of the average stress between two succeeding packages of cycles represents a monotonic load-

ing (Figure 10). It is likely that re-orientations of the grains caused by this monotonic loading erase some parts or the whole memory of the preceding cyclic loading. After sufficiently large monotonic strains the cumulative behaviour of the sand sample during a continued cyclic loading is probably similar to that of a freshly pluviated one, because the cyclic preloading history has been completely forgotten. In the context of the HCA model this means that the preloading variable g^A is reduced or even completely erased (to $g^A = 0$) by a monotonic loading. This effect has not been considered in calculations with the HCA model so far, i.e. the preloading variable g^A has been assumed to continuously increase only.

In a next step, it has been tried out if the cumulative deformations in the multi-stage tests Nos. 2 - 4 can be better reproduced by the HCA model if the memory of the preceding cyclic loading is completely erased at the beginning of each package, i.e. if g^A is set back to zero. The curves provided in cyan colour stem from such simulations. While the strain accumulation rates in tests Nos. 1 and 2 are considerably overestimated by this assumption, the curves predicted for tests Nos. 3 and 4 are closer to the experimental results, in particular in case of the later packages at higher average stress ratios. This gives hints that the sand behaves like a freshly pluviated sample in those packages. However, in case of test No. 2 the memory of the

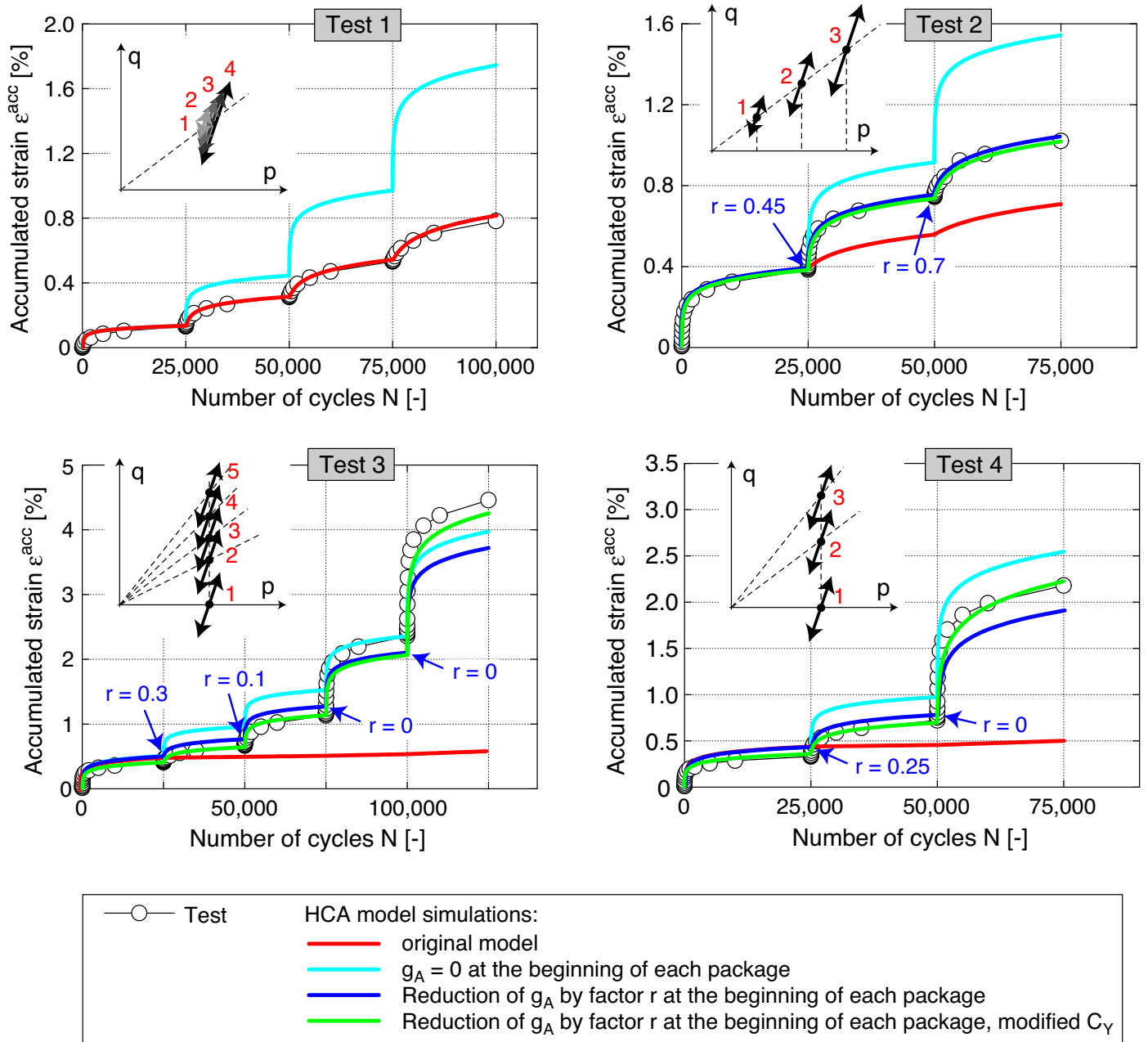


Fig. 9: Accumulation curves $\epsilon^{acc}(N)$ measured in the multi-stage tests with packages of cycles applied with different amplitudes and/or at different average stresses. Only the residual strains caused by the regular cycles are shown (data from first irregular cycle of each package are excluded). The experimental data are supplemented by the curves from simulations with the HCA model, using different assumptions for g^A at the beginning of each package.

cyclic loading history seems not to be fully erased by the monotonic loading phases between the packages.

Subsequently, it has been studied to which extend the preloading variable g^A has to be reduced at the beginning of each subsequent package in order to achieve an optimum reproduction of the experimental curve. A reduction factor r has been introduced, being equal to one if the preloading variable remains unchanged (e.g. in test No. 1, see Figure 9a) and equal to zero if the memory of cyclic preloading history is completely erased. Reduction factors $r = 0.45$ and $r = 0.70$ are appropriate for the second test (see blue curve in Figure 9b), while lower values between 0.3 and 0 are necessary in case of tests Nos. 3 and 4 (blue curves in

Figure 9c,d). A complete loss of memory can be concluded from the parameter $r = 0$ necessary for the packages applied at higher stress ratios. Despite $r = 0$, the residual strains predicted by the HCA model for these later packages are still slightly smaller than those observed in the experiments. An almost perfect agreement with the test data can be achieved if the parameter C_Y of the function f_Y originally calibrated from the 17 single-stage tests is slightly increased (from $C_Y = 2.04$ to 2.6 while simultaneously decreasing C_{N1} from $4.38 \cdot 10^{-4}$ to $3.6 \cdot 10^{-4}$, green curves in Figure 9).

The reduction factors r given in Figure 9 are plotted versus the total strain $\Delta\epsilon$ during the monotonic loading

phases in Figure 11. The residual strain generated during the first (irregular) cycle of each package is incorporated in $\Delta\varepsilon$ because the first quarter of this cycle represents a first (monotonic) loading too, usually leading to much larger plastic strains than the subsequent cycles. It is evident in Figure 11 that a strain of $\Delta\varepsilon \approx 0.4\%$ is sufficient to cause a complete erasure of the cyclic preloading history. The data at smaller values of $\Delta\varepsilon$ show some scatter. In order to work out dependencies between $r(\Delta\varepsilon)$ and factors like stress ratio or density further testing will be undertaken in future.

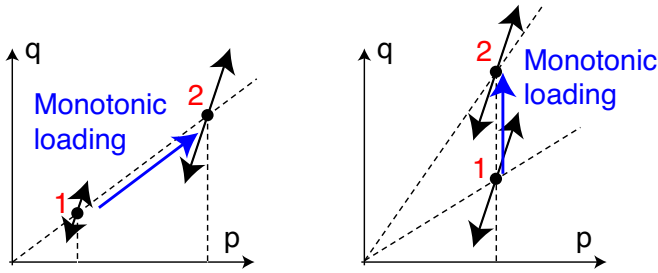


Fig. 10: Monotonic loading due to the change of the average stress between subsequent packages of cycles

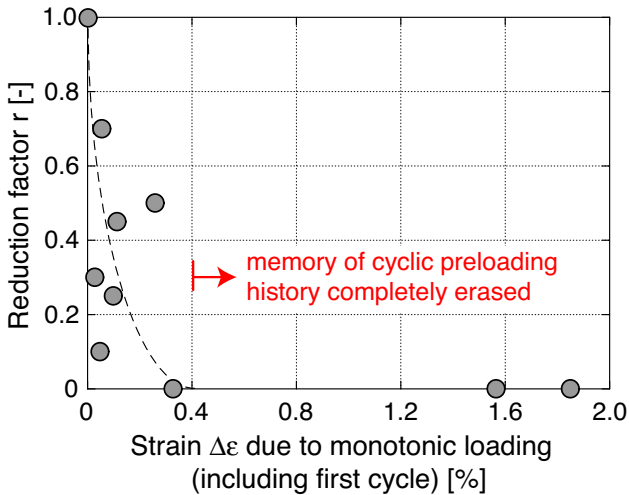


Fig. 11: Reduction factor r for g^A in dependence of strain $\Delta\varepsilon$ during monotonic loading between the packages of cycles

However, the existing test data (Figures 9, 11) already clearly demonstrate that the (partial) loss of the cyclic preloading memory due to monotonic loading may be of great practical relevance for predictions of cumulative deformations if foundations are subjected to a cyclic loading with varying amplitudes and average stresses. Furthermore, a foundation is subjected to a monotonic loading during the construction phase caused by the own weight of the building. This monotonic loading could partially or fully erase the memory of a cyclic loading history of the subsoil, probably leading to larger cumulative deformations during a subsequent cyclic loading of the foundations. Therefore, the conservative assumption $g_0^A = 0$ for the initial state in predictions with the HCA model, usually made because the cyclic preloading of the in situ soil is unknown and no suitable determination method is available yet, may be not as far from reality as previously thought. Beside that, the

observed effect could be utilized for a reduction of the number of cyclic tests necessary for a calibration of the HCA model parameters. If a sample already tested under a certain cyclic loading condition can be reset to a state with $g_0^A = 0$ (similar to a freshly pluviated sample), simply by applying a rather small monotonic loading, several average stresses or amplitudes could be tested in succession on a single sample.

All sequences of average stresses tested in Figure 9 represent a "first loading" in the sense that p^{av} or η^{av} have been increased from bundle to bundle. Further experimental work should also include unloading paths between subsequent packages of cycles. Some experimental studies in the literature give hints that such unloading may dramatically reduce the cumulative rates [14]. Furthermore, another test series performed by the authors (Fig. 2 in [20]) has demonstrated a strong change of the direction of strain accumulation \mathbf{m} (i.e. of the direction of the $\varepsilon_v^{acc} - \varepsilon_q^{acc}$ strain path) after an unloading between subsequent bundles of cycles.

5 Benefits vs. limitations of the HCA model

The test series presented in Section 4 has revealed an effect not captured in simulations with the HCA model yet. This is taken as an occasion to face the advantages and benefits of the HCA model with other known deficits and limitations.

The following advantages or benefits of the HCA model can be addressed:

- The HCA model is based on an extensive data base with cyclic triaxial tests performed on various kinds of granular materials with drained or undrained conditions [30, 32, 33, 37].
- The prediction of the HCA model has been validated based on simulations of element tests, model tests with different scales and field tests [25, 40–43].
- In principle, simulations with the HCA model are not restricted with respect to the number of cycles. However, the simulated number of cycles should not considerably exceed the maximum number of cycles applied in the laboratory tests used as the basis for the calibration of the HCA model parameters.
- The HCA model can be applied to any type of foundation or geotechnical structure. In contrast to more simple engineer-oriented models (e.g. those for monopile foundations of offshore wind turbines [1, 5, 27]) the procedure with the HCA model is not restricted to a certain type of foundation or a certain type of cyclic loading.
- The HCA model does not only allow to predict the development of the permanent deformations with increasing number of cycles, but also to study the complex soil-structure interaction under high-cyclic loading, e.g. changes of the stresses at the contact surfaces between the structure and the soil [43].

The following deficits and limitations of the HCA model should be mentioned:

- A full calibration of the HCA model based on at least 11 drained cyclic triaxial tests is quite laborious.

Therefore, a simplified calibration procedure based on correlations with granulometric or index properties has been developed [33, 37].

- An application of the HCA model is restricted to strain amplitudes lower than $\varepsilon^{\text{ampl}} = 10^{-3}$, because this is the range of strains usually encompassed by cyclic laboratory tests.
- The HCA model in its present form does not accurately describe the deformations due to a monotonic loading applied simultaneously with a cyclic loading. Practically, such monotonic loading can result from redistributions of stresses within a structure caused by a cyclic loading, leading to changes of the average foundation stresses [43]. In a simulation with the HCA model the monotonic loading is also calculated with the elastic stiffness E of the HCA model (see Eq. (1) in Appendix A), which is larger [34, 36] than a typical stiffness for monotonic loading. Therefore, the deformations caused by the monotonic portion of loading may be underestimated.
- The definition of the strain amplitude for multidimensional strain paths incorporated in the HCA model [19] does apply to elliptical paths only. An extension for more complicated paths resulting e.g. from several sources of cyclic loading acting simultaneously or from moving sources (e.g. passing trains) is the matter of current research [20, 31].
- The loss of memory of the cyclic loading history caused by monotonic loading phases is not captured in the HCA model right now, as discussed in Section 4.

6 Summary, conclusions and outlook

In a series of drained cyclic triaxial tests, four amplitudes have been applied in different sequences. In the first part of this series, load signals with amplitudes changing from one cycle to another were tested. In the second part, the same amplitudes were grouped into four or eight packages of cycles each with a constant amplitude. These packages were applied in either an ascending or descending order of the amplitudes. Interestingly, the tests with the bundled amplitudes resulted in slightly larger final residual strains than those with frequently changing amplitudes. Therefore, the bundling of a random cyclic loading into packages of cycles seems conservative. Such bundling is essential for calculations with a high-cycle accumulation (HCA) model. Looking at the tests with packages of cycles, Miner's rule was approximately fulfilled, i.e. the sequence of the amplitudes was of minor importance regarding the final residual deformations. Furthermore, the direction of accumulation, i.e. the ratio of accumulated deviatoric and volumetric strains was found almost unaffected by the various sequences of the amplitudes.

The paper further demonstrates that the HCA model of Niemunis et al. [19] approximately implements both Miner's rule and the approach of Stewart [26], which is frequently cited as a procedure for the handling of packages of cycles when predicting permanent deformations, nowadays in particular in the context of foundations for offshore wind power plants. Other approaches for bundles of cycles as e.g. that recommended in the recommendations for piles "EA Pfähle" [4] have been proven erroneous.

A second series of drained triaxial tests with packages of cycles applied successively at different average stresses revealed an interesting effect: The memory of the sand concerning its cyclic preloading history can be partially or fully erased by a monotonic loading. The cyclic loading leads to subtle changes in the orientations of the grains or grain contacts which render the sand fabric more resistant to subsequent cycles. Substantial reorientations of the grains due to a monotonic loading erase such adaptation of the grain skeleton. In case of the present test series the change of the average stress between subsequent packages of cycles represents such monotonic loading. In the context of the HCA model these findings mean that the variable g^A memorizing the cyclic preloading can be reduced or even fully erased by a monotonic loading. Monotonic strains of about 0.4 % seem to be sufficient to bring g^A back to zero. It has been demonstrated that the HCA model may strongly underestimate the residual strain accumulation in such multi-stage tests if the g^A reduction is not taken into account.

Further testing will be performed in order to quantify the dependence of the g^A reduction on factors like density or the length and direction of the monotonic stress or strain paths between the bundles of cycles.

Acknowledgements

The research presented in this paper was performed within the framework of the project "Improvement of an accumulation model for high-cyclic loading" funded by German Research Council (DFG, project Nos. TR218/18-1/2, WI 3180/3-1/2). The authors are grateful to DFG for the financial support.

References

- [1] M. Achmus, Y.-S. Kuo, and A. Abdel-Rahman. Zur Bemessung von Monopiles für zyklische Lasten. *Der Bauingenieur*, 83:303–311, 2008.
- [2] M. Annaki and K.L. Lee. Equivalent uniform cycle concept for soil dynamics. *Journal of the Geotechnical Engineering Division, ASCE*, 10(GT6):549–564, 1977.
- [3] J. Benoot, W. Haegeman, S. Francois, and G. Degrande. Experimental study of strain accumulation of silica sand in a cyclic triaxial test. In *Proceedings of the 23rd European Young Geotechnical Engineers Conference, Barcelona*, pages 3–6, 2014.
- [4] DGGT. Empfehlungen des Arbeitskreises "Pfähle" der Deutschen Gesellschaft für Geotechnik e.V., 2. Auflage, 2012.
- [5] J. Dührkop. Zum Einfluss von Aufweitungen und zyklischen Lasten auf das Verformungsverhalten lateraler beanspruchter Pfähle in Sand. Dissertation, Veröffentlichungen des Institutes für Geotechnik und Baubetrieb der Technischen Universität Hamburg-Harburg, Heft Nr. 20, 2010.
- [6] K. Ishihara and H. Nagase. Multi-directional irregular loading tests on sand. *Soil Dynamics and Earthquake Engineering*, 7:201–212, 1988.
- [7] K. Ishihara and S. Yasuda. Sand liquefaction due to irregular excitation. *Soils and Foundations*, 12(4):65–77, 1972.
- [8] K. Ishihara and S. Yasuda. Sand liquefaction in hollow cylinder torsion under irregular excitation. *Soils and Foundations*, 15(1):29–45, 1975.

- [9] W.S. Kaggwa, J.R. Booker, and J.P. Carter. Residual strains in calcareous sand due to irregular cyclic loading. *Journal of Geotechnical Engineering, ASCE*, 117(2):201–218, 1991.
- [10] C. Leblanc, B.W. Byrne, and G.T. Houlsby. Response of stiff piles in sand to random two-way lateral loading. *Géotechnique*, 60(9):715–721, 2010.
- [11] C. Leblanc, G.T. Houlsby, and B.W. Byrne. Response of stiff piles in sand to long-term cyclic lateral loading. *Géotechnique*, 60(2):79–90, 2010.
- [12] K.L. Lee and K. Chan. Number of equivalent significant cycles in strong motion earthquakes. In *Proc. Int. Conf. Microzonation for Safer Construction Research and Application*, pages 609–627, 1972.
- [13] S.-S. Lin and J.-C. Liao. Permanent strains of piles in sand due to cyclic lateral loads. *Journal of Geotechnical and Geoenvironmental Engineering, ASCE*, 125(9):798–802, 1999.
- [14] S. López-Querol and M.R. Coop. Drained cyclic behaviour of loose Dogs Bay sand. *Géotechnique*, 62(4):281–289, 2012.
- [15] H. Matsuoaka and T. Nakai. A new failure criterion for soils in three-dimensional stresses. In *Deformation and Failure of Granular Materials*, pages 253–263, 1982. Proc. IUTAM Symp. in Delft.
- [16] M. Miner. Cumulative damage in fatigue. *Transactions of the American Society of Mechanical Engineering*, 67:A159–A164, 1945.
- [17] C.L. Monismith, N. Ogawa, and C.R. Freeme. Permanent deformation characteristics of subgrade soils due to repeated loading. *Transportation Research Record*, 537:1–17, 1975.
- [18] H. Nagase and K. Ishihara. Effects of load irregularity on the cyclic behaviour of sand. *Soil Dynamics and Earthquake Engineering*, 4(6):239–249, 1987.
- [19] A. Niemunis, T. Wichtmann, and T. Triantafyllidis. A high-cycle accumulation model for sand. *Computers and Geotechnics*, 32(4):245–263, 2005.
- [20] A. Niemunis, T. Wichtmann, and Th. Triantafyllidis. On the definition of the fatigue loading for sand. In *International Workshop on Constitutive Modelling - Development, Implementation, Evaluation, and Application, 12-13 January 2007, Hong Kong*, pages 399–404, 2007.
- [21] H.B. Seed. Soil liquefaction and cyclic mobility evaluation for level ground during earthquakes. *Journal of the Geotechnical Engineering Division, ASCE*, 105(GT2):201–255, 1979.
- [22] H.B. Seed and I.M. Idriss. Simplified procedure for evaluating soil liquefaction potential. *Journal of the Soil Mechanics and Foundations Division, ASCE*, 97(SM9):1249–1273, 1971.
- [23] H.B. Seed, I.M. Idriss, F. Makdisi, and N. Banerjee. Representation of irregular stress time histories by equivalent uniform stress series in liquefaction analyses. Technical Report EERC 75-29, Univ. of California, Berkeley, Calif, 1975.
- [24] H.B. Seed, K.L. Lee, and I.M. Idriss. Analysis of the Sheffield dam failure. *Journal of the Soil Mechanics and Foundations Division, ASCE*, 95(SM6):1453–1490, 1969.
- [25] O. Solf. Zum mechanischen Verhalten von zyklisch belasteten Offshore-Gründungen. Dissertation, Veröffentlichungen des Institutes für Bodenmechanik und Felsmechanik am Karlsruher Institut für Technologie, Heft 176, 2012.
- [26] H.E. Stewart. Permanent strains from cyclic variable-amplitude loadings. *Journal of Geotechnical Engineering, ASCE*, 112(6):646–660, 1986.
- [27] H.E. Taşan, F. Rackwitz, and R. Glasenapp. Ein Bemessungsmodell für Monopilegründungen unter zyklischen Horizontallasten. *Bautechnik*, 88(5):301–318, 2011.
- [28] F. Tatsuoka, S. Maeda, K. Ochi, and S. Fujii. Prediction of cyclic undrained strength of sand subjected to irregular loadings. *Soils and Foundations*, 26(2):73–89, 1986.
- [29] J.E. Valera and N.C. Donovan. Soil liquefaction procedures - a review. *Journal of the Geotechnical Engineering Division, ASCE*, 103(GT6):607–625, 1977.
- [30] T. Wichtmann. Explicit accumulation model for non-cohesive soils under cyclic loading. PhD thesis, Publications of the Institute of Soil Mechanics and Foundation Engineering, Ruhr-University Bochum, Issue No. 38, 2005.
- [31] T. Wichtmann. Soil behaviour under cyclic loading - experimental observations, constitutive description and applications. Habilitation thesis, Publications of the Institute of Soil Mechanics and Rock Mechanics, Karlsruhe Institute of Technology, Issue No. 181, 2016.
- [32] T. Wichtmann, A. Niemunis, and T. Triantafyllidis. Strain accumulation in sand due to cyclic loading: drained triaxial tests. *Soil Dynamics and Earthquake Engineering*, 25(12):967–979, 2005.
- [33] T. Wichtmann, A. Niemunis, and T. Triantafyllidis. Validation and calibration of a high-cycle accumulation model based on cyclic triaxial tests on eight sands. *Soils and Foundations*, 49(5):711–728, 2009.
- [34] T. Wichtmann, A. Niemunis, and T. Triantafyllidis. On the "elastic" stiffness in a high-cycle accumulation model for sand: a comparison of drained and undrained cyclic triaxial tests. *Canadian Geotechnical Journal*, 47(7):791–805, 2010.
- [35] T. Wichtmann, A. Niemunis, and T. Triantafyllidis. Strain accumulation in sand due to drained cyclic loading: on the effect of monotonic and cyclic preloading (Miner's rule). *Soil Dynamics and Earthquake Engineering*, 30(8):736–745, 2010.
- [36] T. Wichtmann, A. Niemunis, and T. Triantafyllidis. On the "elastic stiffness" in a high-cycle accumulation model - continued investigations. *Canadian Geotechnical Journal*, 50(12):1260–1272, 2013.
- [37] T. Wichtmann, A. Niemunis, and T. Triantafyllidis. Improved simplified calibration procedure for a high-cycle accumulation model. *Soil Dynamics and Earthquake Engineering*, 70(3):118–132, 2015.
- [38] T. Wichtmann, A. Niemunis, and Th. Triantafyllidis. Gilt die Miner'sche Regel für Sand? *Bautechnik*, 83(5):341–350, 2006.
- [39] T. Wichtmann and Th. Triantafyllidis. Prognose bleibender Verformungen infolge zyklischer Belastung mit veränderlicher Amplitude: Eine Diskussion unterschiedlicher Ansätze. In *Workshop "Gründungen von Offshore-Windenergieanlagen" am 22. und 23. März 2011 in Berlin. Veröffentlichungen des Grundbauinstitutes der Technischen Universität Berlin, Heft Nr. 56, Berlin 2011*, 2011.
- [40] H. Zachert. Zur Gebrauchstauglichkeit von Gründungen für Offshore-Windenergieanlagen. Dissertation, Veröffentlichungen des Institutes für Bodenmechanik und Felsmechanik am Karlsruher Institut für Technologie, Heft Nr. 180, 2015.

- [41] H. Zachert, T. Wichtmann, P. Kudella, T. Triantafyllidis, and U. Hartwig. Validation of a high cycle accumulation model via FE-simulations of a full-scale test on a gravity base foundation for offshore wind turbines. In *International Wind Engineering Conference, IWEC 2014, Hannover*, 2014.
- [42] H. Zachert, T. Wichtmann, T. Triantafyllidis, and U. Hartwig. Simulation of a full-scale test on a Gravity Base Foundation for Offshore Wind Turbines using a High Cycle Accumulation Model. In *3rd International Symposium on Frontiers in Offshore Geotechnics (ISFOG)*, Oslo, 2015.
- [43] H. Zachert, T. Wichtmann, and Th. Triantafyllidis. Soil structure interaction of foundations for offshore wind turbines. In *26th International Ocean and Polar Engineering Conference (ISOPE-2016)*, Rhodes, 2016.

Appendix

Appendix A: Equations of the HCA model

The basic equation of the HCA model reads

$$\dot{\boldsymbol{\sigma}} = \mathbf{E} : (\dot{\boldsymbol{\varepsilon}} - \dot{\boldsymbol{\varepsilon}}^{\text{acc}} - \dot{\boldsymbol{\varepsilon}}^{\text{pl}}) \quad (1)$$

with the stress rate $\dot{\boldsymbol{\sigma}}$ of the effective Cauchy stress $\boldsymbol{\sigma}$ (compression positive), the strain rate $\dot{\boldsymbol{\varepsilon}}$ (compression positive), the accumulation rate $\dot{\boldsymbol{\varepsilon}}^{\text{acc}}$, a plastic strain rate $\dot{\boldsymbol{\varepsilon}}^{\text{pl}}$ (necessary only for stress paths touching the yield surface) and the barotropic elastic stiffness \mathbf{E} . In the context of HCA models the dot over a symbol means a derivative with respect to the number of cycles N (instead of time t), i.e. $\dot{\square} = \partial \square / \partial N$. Depending on the boundary conditions, Eq. (1) predicts either a change of average stress ($\dot{\boldsymbol{\sigma}} \neq \mathbf{0}$) or an accumulation of residual strain ($\dot{\boldsymbol{\varepsilon}} \neq \mathbf{0}$) or both.

For $\dot{\boldsymbol{\varepsilon}}^{\text{acc}}$ in Eq. (1) the following multiplicative approach is used:

$$\dot{\boldsymbol{\varepsilon}}^{\text{acc}} = \dot{\boldsymbol{\varepsilon}}^{\text{acc}} \mathbf{m} \quad (2)$$

with the *direction* of strain accumulation (flow rule) $\mathbf{m} = \dot{\boldsymbol{\varepsilon}}^{\text{acc}} / \|\dot{\boldsymbol{\varepsilon}}^{\text{acc}}\| = (\dot{\boldsymbol{\varepsilon}}^{\text{acc}})^{\rightarrow}$ (unit tensor) and the *intensity* of strain accumulation $\dot{\boldsymbol{\varepsilon}}^{\text{acc}} = \|\dot{\boldsymbol{\varepsilon}}^{\text{acc}}\|$. The flow rule of the modified Cam clay (MCC) model is applied for \mathbf{m} :

$$\mathbf{m} = \left[\frac{1}{3} \left(p^{\text{av}} - \frac{(q^{\text{av}})^2}{M^2 p^{\text{av}}} \right) \mathbf{1} + \frac{3}{M^2} (\boldsymbol{\sigma}^{\text{av}})^* \right]^{\rightarrow} \quad (3)$$

where $\square^{\rightarrow} = \square / \|\square\|$ denotes the normalization of a tensorial quantity. For the triaxial case the critical stress ratio $M = F M_{cc}$ is calculated from

$$F = \begin{cases} 1 + M_{cc}/3 & \text{for } \eta^{\text{av}} \leq M_{cc} \\ 1 + \eta^{\text{av}}/3 & \text{for } M_{cc} < \eta^{\text{av}} < 0 \\ 1 & \text{for } \eta^{\text{av}} \geq 0 \end{cases} \quad (4)$$

wherein

$$M_{cc} = \frac{6 \sin \varphi_{cc}}{3 - \sin \varphi_{cc}} \quad \text{and} \quad M_{cc} = -\frac{6 \sin \varphi_{cc}}{3 + \sin \varphi_{cc}} \quad (5)$$

with parameter φ_{cc} .

The intensity of strain accumulation $\dot{\boldsymbol{\varepsilon}}^{\text{acc}}$ in Eq. (2) is calculated as a product of six functions:

$$\dot{\boldsymbol{\varepsilon}}^{\text{acc}} = f_{\text{ampl}} \dot{f}_N f_e f_p f_Y f_{\pi} \quad (6)$$

each considering a single influencing parameter (see Table 2), i.e. the strain amplitude $\varepsilon^{\text{ampl}}$ (function f_{ampl}), the

Function	Material constants
$f_{\text{ampl}} = \min \left\{ \left(\frac{\varepsilon^{\text{ampl}}}{10^{-4}} \right)^{C_{\text{ampl}}}; 10^{C_{\text{ampl}}} \right\}$	C_{ampl}
$\dot{f}_N = \dot{f}_N^A + \dot{f}_N^B$	C_{N1}
$\dot{f}_N^A = C_{N1} C_{N2} \exp \left[-\frac{g^A}{C_{N1} f_{\text{ampl}}} \right]$	C_{N2}
$\dot{f}_N^B = C_{N1} C_{N3}$	C_{N3}
$f_e = \frac{(C_e - e)^2}{1 + e} \frac{1 + e_{\text{max}}}{(C_e - e_{\text{max}})^2}$	C_e
$f_p = \exp \left[-C_p \left(\frac{p^{\text{av}}}{100 \text{ kPa}} - 1 \right) \right]$	C_p
$f_Y = \exp(C_Y \bar{Y}^{\text{av}})$	C_Y

Table 2: Summary of the functions and material constants of the HCA model

cyclic preloading g^A (\dot{f}_N), void ratio e (f_e), average mean pressure p^{av} (f_p), average stress ratio η^{av} or \bar{Y}^{av} (f_Y) and the effect of polarization changes ($f_{\pi} = 1$ for a constant polarization as in the case of the uniaxial cycles of the test series presented in this paper). The normalized stress ratio \bar{Y}^{av} used in f_Y is zero for isotropic stresses and one on the critical state line. The function Y of Matsuoka & Nakai [15] is used for that purpose:

$$\bar{Y}^{\text{av}} = \frac{Y^{\text{av}} - 9}{Y_c - 9} \quad \text{with} \quad Y_c = \frac{9 - \sin^2 \varphi_{cc}}{1 - \sin^2 \varphi_{cc}} \quad (7)$$

$$Y^{\text{av}} = \frac{27(3 + \eta^{\text{av}})}{(3 + 2\eta^{\text{av}})(3 - \eta^{\text{av}})} \quad (8)$$

For the prediction of strain accumulation due to packages of cycles with different amplitudes the function \dot{f}_N and the preloading variable g^A are of primary importance. In the drained cyclic triaxial tests the curves $\varepsilon^{\text{acc}}(N)$ of the residual strain versus the number of cycles were found to run proportional to the function f_N (compare Figure 9):

$$f_N = C_{N1} [\ln(1 + C_{N2}N) + C_{N3}N] \quad (9)$$

It consists of a logarithmic and a linear portion. The derivative with respect to N is

$$\dot{f}_N = \underbrace{\frac{C_{N1} C_{N2}}{1 + C_{N2}N}}_{\dot{f}_N^A} + \underbrace{C_{N1} C_{N3}}_{\dot{f}_N^B} \quad (10)$$

It can be split into an N -dependent portion \dot{f}_N^A and a constant portion \dot{f}_N^B . However, the number of cycles N alone is not a suitable state variable for the quantification of cyclic preloading (historiotropy) since it contains no information about the intensity of the cycles in the past. A suitable historiotropic variable must consider both, the number *and* the amplitude of the previous cycles. Such variable denoted g^A has been introduced into the HCA model. The derivation of the equations necessary for calculations with g^A is briefly summarized in the following. First, the product of f_{ampl} and \dot{f}_N is denoted as \dot{g} , which can be again split into an N -dependent portion \dot{g}^A and a constant portion \dot{g}^B :

$$\dot{g} = f_{\text{ampl}} \dot{f}_N = f_{\text{ampl}} (\dot{f}_N^A + \dot{f}_N^B)$$

$$= f_{\text{ampl}} \dot{f}_N^A + f_{\text{ampl}} \dot{f}_N^B = \dot{g}^A + \dot{g}^B \quad (11)$$

For the quantification of cyclic preloading only the N -dependent portion \dot{g}^A is of interest. For a cyclic loading with constant strain amplitude ($f_{\text{ampl}} = \text{constant}$), the preloading variable g^A can be obtained by integration as follows:

$$\begin{aligned} g^A &= \int \dot{g}^A dN = \int f_{\text{ampl}} \dot{f}_N^A dN \\ &= f_{\text{ampl}} C_{N1} \ln(1 + C_{N2} N) \end{aligned} \quad (12)$$

If this equation is rearranged for N , one obtains:

$$N = \frac{1}{C_{N2}} \left[\exp\left(\frac{g^A}{f_{\text{ampl}} C_{N1}}\right) - 1 \right] \quad (13)$$

Setting Eq. (13) in \dot{f}_N^A according to Eq. (10) delivers the expression for \dot{f}_N^A given in Table 2:

$$\dot{f}_N^A = C_{N1} C_{N2} \exp\left(-\frac{g^A}{f_{\text{ampl}} C_{N1}}\right) \quad (14)$$

and thus a relationship between the rate and the actual value of the preloading variable:

$$\dot{g}^A = f_{\text{ampl}} C_{N1} C_{N2} \exp\left(-\frac{g^A}{f_{\text{ampl}} C_{N1}}\right) \quad (15)$$

The rate of g^B is independent of cyclic preloading:

$$\dot{g}^B = f_{\text{ampl}} C_{N1} C_{N3} \quad (16)$$

In the following, the procedure for an incremental calculation with the HCA model is briefly demonstrated by means of a drained triaxial test with stress cycles. Only the total strain ε^{acc} is considered. First, an initial value for g^A has to be chosen. For a freshly pluviated sample the choice of $g_0^A = 0$ is justified. For each increment ΔN of the number of cycles the calculation procedure is as follows:

1. Calculation of \dot{f}_N^A from Eq. (14) with the actual value of the preloading variable g^A , calculation of $\dot{f}_N^B = C_{N1} C_{N3}$ and $\dot{f}_N = \dot{f}_N^A + \dot{f}_N^B$
2. Calculation of the intensity of strain accumulation $\dot{\varepsilon}^{\text{acc}}$ from Eq. (6)
3. For the drained case $\dot{\varepsilon} = \dot{\varepsilon}^{\text{acc}}$ follows from Eq. (1)
4. Calculation of the strain increment $\Delta \varepsilon = \dot{\varepsilon} \Delta N$, update of strain $\varepsilon(N + \Delta N) = \varepsilon(N) + \Delta \varepsilon$
5. Calculation of the rate of the preloading variable \dot{g}^A from Eq. (15) with the actual value of g^A
6. Calculation of the increment of the preloading variable $\Delta g^A = \dot{g}^A \Delta N$, update of the preloading variable $g^A(N + \Delta N) = g^A(N) + \Delta g^A$. This updated preloading variable enters the calculation of the next increment ΔN .

Appendix B: Equations of the approach of Stewart [26]

If the accumulation of strain due to N_i cycles with amplitude "i" is described by a logarithmic function

$$\varepsilon_i^{\text{acc}}(N_i) = \varepsilon_i^{\text{acc}}(N = 1)[1 + t \ln(N_i)] \quad (17)$$

with the residual strain $\varepsilon_i^{\text{acc}}(N = 1)$ due to the first cycle and a parameter t , then the residual strains $\varepsilon_1^{\text{acc}}$, $\varepsilon_2^{\text{acc}}$ and $\varepsilon_3^{\text{acc}}$ after the first, second and third package with the numbers of cycles N_1 , N_2 and N_3 are calculated as follows:

$$\begin{aligned} \varepsilon_1^{\text{acc}} &= \varepsilon_1^{\text{acc}}(N = 1)[1 + t \ln(N_1)] \\ N_{1,2}^* &= \exp\left\{\frac{1}{t} \left[\frac{\varepsilon_1^{\text{acc}}}{\varepsilon_2^{\text{acc}}(N = 1)} - 1 \right]\right\} \\ &= \exp\left\{\frac{1}{t} \left[\frac{\varepsilon_1^{\text{acc}}(N = 1)[1 + t \ln(N_1)]}{\varepsilon_2^{\text{acc}}(N = 1)} - 1 \right]\right\} \\ \varepsilon_2^{\text{acc}} &= \varepsilon_2^{\text{acc}}(N = 1)[1 + t \ln(N_{1,2}^* + N_2)] \\ &= \varepsilon_2^{\text{acc}}(N = 1)[1 + t \ln(N_{2,\text{eq}})] \\ N_{2,3}^* &= \exp\left\{\frac{1}{t} \left[\frac{\varepsilon_2^{\text{acc}}}{\varepsilon_3^{\text{acc}}(N = 1)} - 1 \right]\right\} \\ &= \exp\left\{\frac{1}{t} \left[\frac{\varepsilon_2^{\text{acc}}(N = 1)[1 + t \ln(N_{1,2}^* + N_2)]}{\varepsilon_3^{\text{acc}}(N = 1)} - 1 \right]\right\} \\ \varepsilon_3^{\text{acc}} &= \varepsilon_3^{\text{acc}}(N = 1)[1 + t \ln(N_{2,3}^* + N_3)] \\ &= \varepsilon_3^{\text{acc}}(N = 1)[1 + t \ln(N_{3,\text{eq}})] \end{aligned}$$

For i packages of cycles the equations generally read:

$$\begin{aligned} N_{i-1,i}^* &= \exp\left\{\frac{1}{t} \left[\frac{\varepsilon_{i-1}^{\text{acc}}}{\varepsilon_i^{\text{acc}}(N = 1)} - 1 \right]\right\} \\ &= \exp\left\{\frac{1}{t} \left[\frac{\varepsilon_{i-1}^{\text{acc}}(N = 1)[1 + t \ln(N_{i-2,i-1}^* + N_{i-1})]}{\varepsilon_i^{\text{acc}}(N = 1)} - 1 \right]\right\} \end{aligned} \quad (18)$$

$$\begin{aligned} \varepsilon_i^{\text{acc}} &= \varepsilon_i^{\text{acc}}(N = 1)[1 + t \ln(N_{i-1,i}^* + N_i)] \\ &= \varepsilon_i^{\text{acc}}(N = 1)[1 + t \ln(N_{i,\text{eq}})] \end{aligned} \quad (19)$$

If a power law relationship

$$\varepsilon_i^{\text{acc}}(N_i) = \varepsilon_i^{\text{acc}}(N = 1)(N_i)^\alpha \quad (20)$$

is applied instead of the logarithmic function, then the recursive formulas for the equivalent number of cycles $N_{i-1,i}^*$ and for the residual strain $\varepsilon_i^{\text{acc}}$ after i packages of cycles read:

$$\begin{aligned} N_{i-1,i}^* &= \left(\frac{\varepsilon_{i-1}^{\text{acc}}}{\varepsilon_i^{\text{acc}}(N = 1)}\right)^{1/\alpha} \\ &= \left(\frac{\varepsilon_{i-1}^{\text{acc}}(N = 1)}{\varepsilon_i^{\text{acc}}(N = 1)}\right)^{1/\alpha} (N_{i-2,i-1}^* + N_{i-1}) \end{aligned} \quad (21)$$

$$\varepsilon_i^{\text{acc}} = \varepsilon_i^{\text{acc}}(N = 1)(N_{i-1,i}^* + N_i)^\alpha \quad (22)$$

Appendix C: Equations of recommendations for piles "EA Pfähle" [4]

The procedure proposed in the recommendations "EA Pfähle" [4] for piles under horizontal cyclic loading is explained on the basis of the logarithmic function (17). Although the equations are given in terms of the lateral pile head deflection y in [4], for the sake of consistency within this paper, they are written in terms of an accumulated strain ε^{acc} in the following. According to [4] a reference amplitude has to be chosen, which is denoted by the index "ref". All other amplitudes (numbered from 1 to k) are referred to this reference value. The accumulated strain due

to $k + 1$ packages of cycles is obtained from:

$$\begin{aligned}\varepsilon_{\text{ref}}^{\text{acc}} &= \varepsilon_{\text{ref}}^{\text{acc}}(N = 1) \left[1 + t \ln \left(N_{\text{ref}} + \sum_{i=1}^k N_{i,\text{ref}}^* \right) \right] \\ &= \varepsilon_{\text{ref}}^{\text{acc}}(N = 1) [1 + t \ln(N_{\text{ref},\text{eq}})]\end{aligned}\quad (23)$$

with

$$N_{i,\text{ref}}^* = \exp \left\{ \frac{1}{t} \left[\frac{\varepsilon_i^{\text{acc}}(N = 1)[1 + t \ln(N_i)]}{\varepsilon_{\text{ref}}^{\text{acc}}(N = 1)} - 1 \right] \right\} \quad (24)$$

In [4] the equations (23) and (24) are addressed as implementation of the concept of Stewart [26]. However, it can be easily demonstrated that this is not correct.

For two packages with the number of cycles N_1 and N_2 and the residual strains $\varepsilon_1^{\text{acc}}(N = 1)$ and $\varepsilon_2^{\text{acc}}(N = 1)$ after the first cycle, Eqs. (23) and (24) lead to the same solution as Eqs. (18) and (19) if amplitude 2 is used as reference:

$$\begin{aligned}N_{1,2}^* &= \exp \left\{ \frac{1}{t} \left[\frac{\varepsilon_1^{\text{acc}}(N = 1)[1 + t \ln(N_1)]}{\varepsilon_2^{\text{acc}}(N = 1)} - 1 \right] \right\} \\ \varepsilon_2^{\text{acc}} &= \varepsilon_2^{\text{acc}}(N = 1) [1 + t \ln(N_{1,2}^* + N_2)] \\ &= \varepsilon_2^{\text{acc}}(N = 1) [1 + t \ln(N_{2,\text{eq}})]\end{aligned}$$

For three or more packages of cycles, however, the solutions of Eqs. (23) and (24) differ from those of Eqs. (18) and (19). Considering three packages of cycles and choosing the amplitude of the third package as reference, one obtains:

$$\begin{aligned}N_{1,3}^* &= \exp \left\{ \frac{1}{t} \left[\frac{\varepsilon_1^{\text{acc}}(N = 1)[1 + t \ln(N_1)]}{\varepsilon_3^{\text{acc}}(N = 1)} - 1 \right] \right\} \\ N_{2,3}^* &= \exp \left\{ \frac{1}{t} \left[\frac{\varepsilon_2^{\text{acc}}(N = 1)[1 + t \ln(N_2)]}{\varepsilon_3^{\text{acc}}(N = 1)} - 1 \right] \right\} \\ \varepsilon_3^{\text{acc}} &= \varepsilon_3^{\text{acc}}(N = 1) [1 + t \ln(N_{1,3}^* + N_{2,3}^* + N_3)] \\ &= \varepsilon_3^{\text{acc}}(N = 1) [1 + t \ln(N_{3,\text{eq}})]\end{aligned}$$

A graphical presentation of Eqs. (23) and (24) for three packages of cycles with ascending order of amplitudes and choosing the largest amplitude 3 as reference is given in Figure 5a. As evident in Figure 5a, all packages of cycles with amplitudes differing from the reference one are treated separately. The residual strain $\varepsilon_1^{\text{acc}}$ resulting from N_1 cycles with amplitude 1 is converted into an equivalent number of cycles $N_{1,3}^*$ referring to amplitude 3. Analogously, the residual strain $\varepsilon_2^{\text{acc}}$ due to N_2 cycles with amplitude 2 results in $N_{2,3}^*$. In contrast to the approach of Stewart (Appendix B) the cyclic preloading due to the N_1 cycles with amplitude 1 is not considered when evaluating $N_{2,3}^*$. Finally, $N_{1,3}^*$, $N_{2,3}^*$ and the number of cycles N_3 applied with the reference amplitude are added. The resulting residual strain is calculated as the result of $N_{1,3}^* + N_{2,3}^* + N_3$ cycles with amplitude 3.

Appendix D: Example in Figure 6 - By hand calculation with the HCA model following the approach of Stewart [26]

The HCA model parameters in Table 3 have been used for the example in Figure 6. For a relative density $I_D = 0.6$ (corresponds to a void ratio $e = 0.828$) one obtains a value of $f_e = 0.283$ for the void ratio function. The average stress with $p^{\text{av}} = 200$ kPa and $\eta^{\text{av}} = 0.75$ leads to $f_p = 0.787$ and

C_{ampl}	C_e	C_p	C_Y	C_{N1}	C_{N2}	C_{N3}
1.32	0.60	0.24	1.74	$3.03 \cdot 10^{-4}$	0.37	$2.36 \cdot 10^{-5}$

Table 3: HCA model parameters of Karlsruhe fine sand ($e_{\text{min}} = 0.677$, $e_{\text{max}} = 1.054$)

$f_Y = 1.668$. In this example the functions f_e , f_p and f_Y are assumed constant.

The three packages of cycles according to Table 4 have been applied in ascending order. If a freshly pluviated sample would be loaded with the constant amplitude $\varepsilon_1^{\text{ampl}}$ of the first package of cycles, one would obtain a development of the residual strain with increasing number of cycles according to the red curve in Figure 6:

$$\begin{aligned}\varepsilon^{\text{acc}}(N) &= f_{\text{ampl}} f_e f_p f_Y f_N \\ &= 2.497 \cdot 0.283 \cdot 0.787 \cdot 1.668 \cdot 3.03 \cdot 10^{-4} \\ &\quad \cdot [\ln(1 + 0.37 \cdot N) + 2.36 \cdot 10^{-5} \cdot N] \\ &= 2.81 \cdot 10^{-4} \cdot [\ln(1 + 0.37 \cdot N) + 2.36 \cdot 10^{-5} \cdot N]\end{aligned}$$

Analogously, a freshly pluviated sample loaded with amplitude 2 would be compacted according to (blue curve in Figure 6):

$$\varepsilon^{\text{acc}}(N) = 7.02 \cdot 10^{-4} \cdot [\ln(1 + 0.37 \cdot N) + 2.36 \cdot 10^{-5} \cdot N]$$

For amplitude 3 (green curve in Figure 6) one obtains:

$$\varepsilon^{\text{acc}}(N) = 11.98 \cdot 10^{-4} \cdot [\ln(1 + 0.37 \cdot N) + 2.36 \cdot 10^{-5} \cdot N]$$

The residual strains $\varepsilon_1^{\text{acc}}$, $\varepsilon_2^{\text{acc}}$ and $\varepsilon_3^{\text{acc}}$ after the packages of cycles Nos. 1, 2 and 3 result from the following equations:

$$\begin{aligned}\varepsilon_1^{\text{acc}} &= 2.81 \cdot 10^{-4} \cdot [\ln(1 + 0.37 \cdot 10000) \\ &\quad + 2.36 \cdot 10^{-5} \cdot 10000] = 0.238 \% \\ 0.238 \% &= 7.02 \cdot 10^{-4} \cdot [\ln(1 + 0.37 \cdot N_{1,2}^*) \\ &\quad + 2.36 \cdot 10^{-5} \cdot N_{1,2}^*] \rightarrow N_{1,2}^* = 77.0 \\ \varepsilon_2^{\text{acc}} &= 7.02 \cdot 10^{-4} \cdot [\ln(1 + 0.37 \cdot (N_{1,2}^* + N_2)) \\ &\quad + 2.36 \cdot 10^{-5} \cdot (N_{1,2}^* + N_2)] \\ &= 7.02 \cdot 10^{-4} \cdot [\ln(1 + 0.37 \cdot (77.0 + 5000)) \\ &\quad + 2.36 \cdot 10^{-5} \cdot (77.0 + 5000)] = 0.537 \% \\ 0.537 \% &= 11.89 \cdot 10^{-4} \cdot [\ln(1 + 0.37 \cdot N_{2,3}^*) \\ &\quad + 2.36 \cdot 10^{-5} \cdot N_{2,3}^*] \rightarrow N_{2,3}^* = 235.5 \\ \varepsilon_3^{\text{acc}} &= 11.98 \cdot 10^{-4} \cdot [\ln(1 + 0.37 \cdot (N_{2,3}^* + N_3)) \\ &\quad + 2.36 \cdot 10^{-5} \cdot (N_{2,3}^* + N_3)] \\ &= 11.98 \cdot 10^{-4} \cdot [\ln(1 + 0.37 \cdot (235.5 + 1000)) \\ &\quad + 2.36 \cdot 10^{-5} \cdot (235.5 + 1000)] = 0.738 \%\end{aligned}$$

The analogous calculation with descending amplitudes delivers $\varepsilon_1^{\text{acc}} = 0.712$ %, $\varepsilon_2^{\text{acc}} = 0.730$ % and $\varepsilon_3^{\text{acc}} = 0.737$ %. Therefore, the residual strain at the end of the third package of cycles is almost identical for an ascending and a descending order of the amplitudes.

Appendix E: By hand calculation with the exact equations of the HCA model

The by hand calculation according to Stewart [26] presented in Figures 6 and 7 reproduces the residual strain

Package No	Number of cycles N_i	Strain amplitude $\varepsilon_i^{\text{ampl}}$	Amplitude function f_i^{ampl}
1	10000	$2 \cdot 10^{-4}$	2.497
2	5000	$4 \cdot 10^{-4}$	6.233
3	1000	$6 \cdot 10^{-4}$	10.645

Table 4: Packages of cycles considered in the example in Figure 6

predicted by the HCA model only approximatively. The reason is explained below. In the following, the exact equations for a by hand calculation of packages of cycles using the HCA model are presented. Two different strategies can be distinguished, one using the preloading variable g_i^A and the other one an equivalent number of cycles $N_{i-1,i}^*$ [39].

First, the equations in terms of g_i^A are provided. The preloading variable g_i^A at the end of a package i can be calculated from the preloading variable g_{i-1}^A at the beginning of that package, the amplitude function $f_{\text{ampl},i}$ and the number of cycles N_i of the package:

$$g_i^A = f_{\text{ampl},i} C_{N1} \ln \left[\exp \left(\frac{g_{i-1}^A}{C_{N1} f_{\text{ampl},i}} \right) + C_{N2} N_i \right] \quad (25)$$

The increase of the residual strain due to the package i is then obtained from:

$$\begin{aligned} \Delta \varepsilon_i^{\text{acc}} = & f_e f_p f_Y \left\{ g_i^A - g_{i-1}^A + \frac{C_{N1} C_{N3}}{C_{N2}} f_{\text{ampl},i} \cdot \right. \\ & \left. \cdot \left[\exp \left(\frac{g_i^A}{f_{\text{ampl},i} C_{N1}} \right) - \exp \left(\frac{g_{i-1}^A}{f_{\text{ampl},i} C_{N1}} \right) \right] \right\} \quad (26) \end{aligned}$$

and the residual strain at the end of package i is:

$$\varepsilon_i^{\text{acc}} = \varepsilon_{i-1}^{\text{acc}} + \Delta \varepsilon_i^{\text{acc}} \quad (27)$$

The equivalent number of cycles $N_{i-1,i}^*$ is introduced as follows:

$$g_i^A = f_{\text{ampl},i} C_{N1} \ln [1 + C_{N2} (N_i + N_{i-1,i}^*)] \quad (28)$$

The equivalent number of cycles $N_{i-1,i}^*$ according to Eq. (28) considers the N -dependent portion of the rate of strain accumulation only. In contrast, the procedure of Stewart [26] does not distinguish between N -dependent and N -independent parts of the strain accumulation curve, leading to the deviations from the HCA model prediction visible in Figure 7. The equivalent number of cycles at the end of package $i-1$, referring to the amplitude of the next package i reads:

$$N_{i-1,i}^* = \frac{1}{C_{N2}} \left\{ [1 + C_{N2} (N_{i-1} + N_{i-2,i-1}^*)] \frac{f_{\text{ampl},i-1}}{f_{\text{ampl},i}} - 1 \right\} \quad (29)$$

The increase of strain due to package i is then calculated from:

$$\begin{aligned} \Delta \varepsilon_i^{\text{acc}} = & f_e f_p f_Y C_{N1} \{ \\ & - f_{\text{ampl},i-1} \ln [1 + C_{N2} (N_{i-1} + N_{i-2,i-1}^*)] \\ & + f_{\text{ampl},i} [\ln [1 + C_{N2} (N_i + N_{i-1,i}^*)] + C_{N3} N_i] \} \quad (30) \end{aligned}$$

The residual strain at the end of package i is:

$$\begin{aligned} \varepsilon_i^{\text{acc}} = & f_e f_p f_Y C_{N1} \left[\left(\sum_1^i f_{\text{ampl},i} C_{N3} N_i \right) \right. \\ & \left. + f_{\text{ampl},i} \ln (1 + C_{N2} (N_i + N_{i-1,i}^*)) \right] \quad (31) \end{aligned}$$

Examples for a calculation with both sets of equations, using either g_i^A or $N_{i-1,i}^*$, are provided in [39].